Solar Energy Materials & Solar Cells 93 (2009) 684–690

Contents lists available at ScienceDirect

Solar Energy Materials & Solar Cells

journal homepage: www.elsevier.com/locate/solmat

n-Type silicon quantum dots and p-type crystalline silicon heteroface solar cells

Sangwook Park *, Eunchel Cho, Dengyuan Song, Gavin Conibeer, Martin A. Green

ARC Photovoltaics Centre of Excellence, University of New South Wales, Sydney, NSW 2052, Australia

A R T I C L E I N F O

Article history:
Received 6 January 2008
Accepted 17 September 2008
Available online 17 November 2008

Keywords:
Nanostructure
Quantum dot
Photovoltaics
Third generation

A B S T R A C T

Heteroface devices have been realized by depositing phosphorus-doped silicon (Si) quantum dots (QDs) (n-type) on a p-type crystalline silicon substrate. To compare the quantum confinement effect, different sizes (3, 4, 5, and 8 $\pm$ 1 nm) of Si QD were fabricated, whose optical energy bandgaps are in the ranges of 1.3–1.65 eV. The electrical and photovoltaic properties of heterojunction devices were characterized by illuminated and dark *I–V* measurements, *C–V* measurements, and spectral response measurements. The diodes showed a good rectification ratio of 5×10^6 for 4 nm Si QDs at the bias voltage of $\pm$1.0 V at 298 K. The ideality factor and junction built-in potential deduced from current–voltage (*I–V*) and capacitance–voltage (*C–V*) plots are 1.86 and 0.847 V for 3 nm QD device, respectively. From the illuminated *IV* characteristics, the open circuit voltages were 556, 540, 512, and 470 mV for mean QD diameters 3, 4, 5, and 8 $\pm$ 1 nm, respectively. Temperature-dependant dark *I–V* measurements suggest that the carrier transport in the devices is controlled by recombination in the space-charge region. This study indicates the silicon QDs can be good candidates for all-silicon tandem solar cells.

1. Introduction

The two most important power loss mechanisms in single bandgap solar cells are longer energy less than bandgap and shorter energy greater than bandgap [1]. Longer wavelength is not absorbed by the solar cell material. Shorter wavelength generates an electron–hole pair greater than the bandgap of the pn junction material. The excess energy is lost as heat because the electron (and hole) relaxes to the conduction (and valence) band edge. The amounts of the losses are around 23% and 33% of the incoming solar energies, respectively [2]. Other losses are junction loss, contact loss, and recombination loss. To use full solar spectrum, several techniques were proposed [3]. One of the approaches for improving efficiency beyond that of a standard pn junction cell is to use a tandem stack of cells, with a stack of a different bandgap material. The efficiency limit for a single pn junction cell is 29%, but this increases to 42.5% and 47.5% for 2-cell and 3-cell tandem solar cells, respectively [2]. One of the proposed materials for all-silicon tandem cell is silicon (Si) quantum dot (QD) superlattices [4,5]. By restricting the dimensions of silicon to less than Bohr radius of bulk crystalline silicon (~5 nm), quantum confinement causes its effective bandgap to increase. If these dots are close together, carriers can tunnel between them to produce QD superlattices. Such superlattices can then be used as the higher bandgap materials in a tandem cell. Silicon is unique in that it has an almost ideal bandgap not only for a standard single pn junction cell (just a little on the low side of optimal) but also for the lower cell in a 2-cell or even a 3-cell tandem stack (a little on the high side). The optimal bandgap of the top cell to maximize conversion efficiency is 1.7–1.8 eV for 2-cell tandem with a Si bottom cell. Effective bandgap of newly synthesized Si QD dispersed in oxide was demonstrated up to 1.7 eV for a dot diameter about 2 nm by measuring photoluminescence [3].

As a first step to realize all-silicon tandem solar cells, we fabricated phosphorus-doped Si QDs superlattice as an active layer on p-type crystalline Si (c-Si) substrate as shown in Fig. 1. The phosphorous doping in n-type Si QDs superlattice was realized by P_2O_5 co-sputtering during the deposition of silicon-rich oxide (SRO, Si and SiO_2 co-sputtering), which forms Si QDs upon high-temperature post-annealing. The n-type region typically includes 15 or 25 bi-layers formed by alternating deposition of P-doped QDs and SiO_2. This paper concentrates on Si QDs/c-Si heterojunction solar cells without high-efficiency features such as surface texturing, anti reflection coating, and back-surface field. We first describe the preparation steps for our heteroface solar cells. The structural characterisations were accomplished by transmission electron microscopy (TEM) and Raman spectroscopy. To clarify the effect of annealing on impurity redistribution of devices, SIMS measurement was used to investigate the depth profile of the dopant (phosphorus) across the heteroface interface.

* Corresponding author. Tel.: +61 2 9385 6052; fax: +61 2 9385 5104.
E-mail address: sangwook.park@student.unsw.edu.au (S. Park).

0927-0248/$ - see front matter © 2008 Elsevier B.V. All rights reserved.
doi:10.1016/j.solmat.2008.09.032

The optical bandgap energy (E_{opt}) of films was determined by Tauc's equation. The electronic and photovoltaic properties of the heteroface devices were characterised by illuminated and dark current–density–voltage characterisation, spectral response, and capacitance–voltage (*C–V*) measurements.

2. Experiments

One-side-polished p-type CZ silicon wafers with an average resistivity of 5–20 Ω cm (N_A~3×10^{15}–7×10^{14} cm^{-3}) were used as a substrate. As a first preparation step to fabricate the hetero-junction solar cells, the c-Si wafers were cleaned by piranha cleaning solution (3:1 H_2SO_4:H_2O_2) and rinsed in deionized water. Secondly the native oxide was removed from the Si wafers by a dilute (5%) HF. Immediately after oxide removal, the c-Si substrates were transferred into the loadlock chamber of a computer-controlled AJA ATC-2200 system. Prior to deposition, the sputtering chamber was evacuated to a base pressure of ~3×10^{-7} Torr. Argon (Ar) was then introduced into the chamber to establish a working pressure of 1.5 mTorr, which was maintained throughout the film deposition.

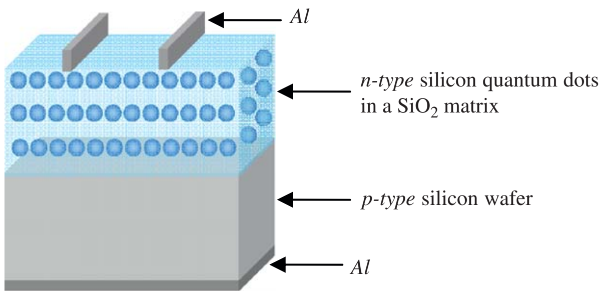

Fig. 1. Schematic diagram of (n-type) Si QDs and (p-type) c-Si heterojunction solar cell.

Phosphorus-doped n-type Si QDs layer was prepared by a co-sputtering of silicon, quartz, and P_2O_5 targets at room temperature without addition of oxygen .The concentration of phosphorus in the SRO was controlled by the deposition rates of three targets and was around 0.23 at%. The n-type region consisted of 15 or 25 layers of the Si QDs in an oxide matrix with layer thicknesses 3, 4, 5, and 8 ± 1 nm to compare quantum confinement effect due to difference in dot sizes. Si QDs were precipitated during a high-temperature post-annealing at 1100 °C for 1 h in a nitrogen atmosphere. Aluminium was evaporated through a shadow mask onto the front of the solar cell, and full back area of the cell. Then the samples were sintered at 400 °C for 30 min to ensure a good ohmic contact. The area of devices was 1.0 × 1.0 cm^2.

The films were investigated by cross-sectional TEM of a JEOL-3000F with incident electron energy of 300 kV. Raman spectra were measured by a micro-Raman spectrometer (Renishaw, In-Via) in a backscattering configuration, with a 50× optical microscope objective. The laser light comes from an Ar ion laser with a wavelength of 514.5 nm. The SIMS analysis was done by a 25 kV Bi^+ time-of-flight SIMS (TOF-SIMS) IV system, ION-TOF with sputtering of 0.5 kV Cs^+ ions at a 45° incident angle. The beam currents were 1 pA and 30 nA for analysis gun and sputtering gun, respectively. A double-beam UV/visible/IR spectrophotometer (Varian Cary 5G) and an attached integrating sphere (Labsphere, RSA-CA-50) were used to measure transmission and reflection spectra. The 1-Sun *I–V* characteristics were measured by an

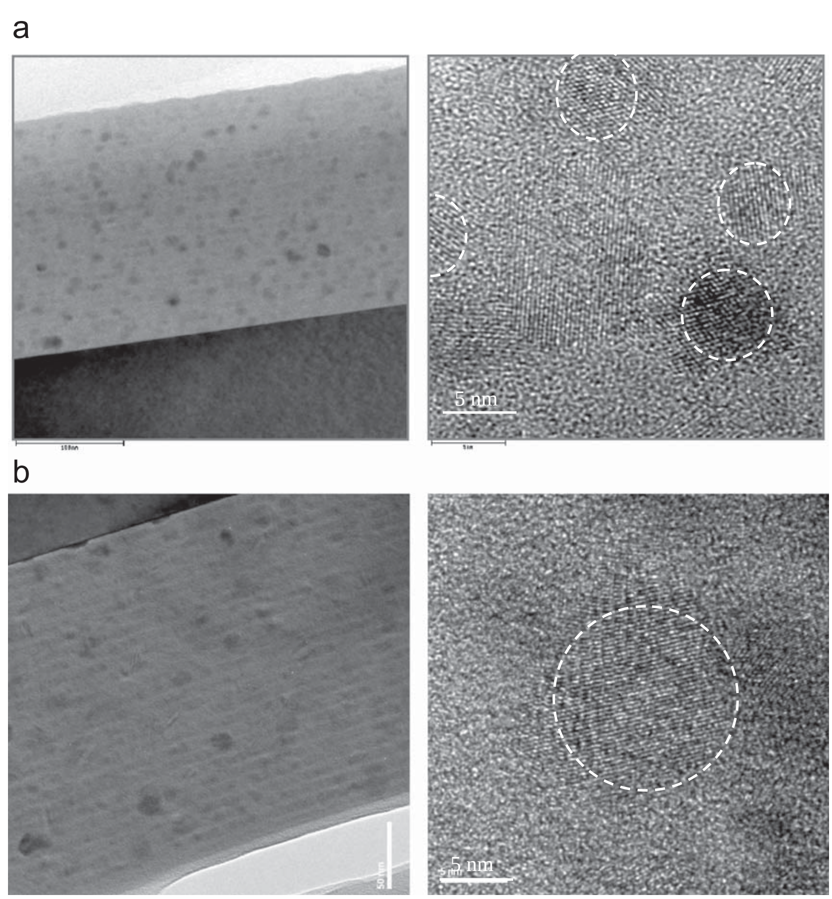

Fig. 2. Transmission electron microscopy (TEM) images of Si quantum dots in SiO_2 matrix with low-magnification and high-resolution lattice images for (a) 5 nm Si QDs and (b) 8 ± 1 nm Si QDs.